SUPERCONDUCTIVITY IN AMORPHOUS TRANSITION METAL THIN FILMS

by

Robert Arthur Lacy

Department of Physics

Submitted in Partial Fulfillment of the Requirement of the

University Undergraduate Fellows Program

1977 - 1978

Approved by:

Donald G. Naugle

Dr. Donald G. Naugle

April 1978

ABSTRACT

The superconducting transition temperature of a $La_{.80}Ga_{.20}$ alloy thin film prepared by the vapor-quench technique has been measured. An annealing curve of film resistivity as a function of temperature is inconclusive as to whether or not the film was amorphous.

ACKNOWLEDGMENTS

The author would like to thank his faculty advisor, Dr. Donald Naugle, for his advice and guidance during this project. The author would also like to thank Gary Cort for the many evenings spent in preparing the helium cryostat for the transition temperature measurements.

TABLE OF CONTENTS

LIST OF FIGURES

I. Introduction*

The phenomenon of superconductivity has been known for more than half a century, having been first observed by Heike Kamerlingh Onnes in 1911. Historically, solid state theory developed from assumptions of regular crystal structure, and the most developed theories of superconductivity are based upon the interaction of conduction electrons with a periodic crystal lattice. These theories are inadequate to explain the phenomenon of superconductivity in highly disordered or amorphous metals. Since Buckel and Hilsch[1] demonstrated the existence of amorphous superconductors, considerable interest has focussed on the properties of amorphous transition metals, whose behavior is more interesting than that of amorphous simple metals.[2] Although progress towards understanding the behavior of amorphous transition metals has been made, a complete understanding has been hindered in part by the scarcity of experimental data.

One of the earliest systematic studies in this field was that Collver and Hammond,[3] in which it was shown that for 4d and 5d transition metal alloy amorphous films, T_c shows a smooth triangular variation as a function of the average number of valence electrons per atom, $\frac{e}{a}$. (See Fig. 1.) This is in sharp contrast to the behavior of T_c for crystalline transition metal alloy films, in which case T_c is predominantly influenced by the crystal structure of the film, with a sharp minimum in T_c for $\frac{e}{a} \simeq 6$. This sharp minimum

---

*This paper follows the format of the Physical Review.

has been explained[4] as due to the formation of directed d-bonds in the crystal lattice, which inhibit superconductivity. These highly directional d-bonds cannot form in amorphous films due to the disorder of the atoms, and hence we see an enhancement of T_c for amorphous transition metal alloys with $\frac{e}{a}$ in the approximate range of 5 to 7.

The author's original goal was to perform a systematic study of T_c as a function of $\frac{e}{a}$ for a binary alloy, and to compare the results with those of Collver and Hammond. Recent studies[5] of amorphous $La_{1-x}Ga_x$ and $La_{1-x}Au_x$ films produced by the "splat cooling" technique[6] have shown such samples to remain amorphous at room temperature for periods of several days. This is exceptional behavior for amorphous metals, most of which undergo a phase transition to the crystalline state at well below room temperature. The necessity of working with a metastable amorphous alloy led the author to choose the $La_{1-x}Ga_x$ system for study. However, the number of valence electrons of both La and Ga is three, making variations in $\frac{e}{a}$ impossible. The construction of apparatus to permit the use of a wider range of alloys by making transition temperature measurements in situ was unfortunately beyond the scope of this research.

II. Experimental Details

A. Quartz Crystal Microbalance for Film Thickness Measurements

The production of thin films by condensing metal vapor onto a substrate in a vacuum has applications ranging from anti-reflection coatings on lenses to the production of electronic components. One generally desires precise control of film thickness and rate of deposition during the actual evaporation. In 1957, Sauerbrey[7] showed theoretically that if one deposited a thin film onto the surface of a quartz oscillator crystal, the shift in the resonant frequency of the crystal should be proportional to the mass of the film, provided that the mass of the film is very small compared to the mass of the crystal. The use of quartz crystal oscillators to measure film thicknesses has become a highly refined technique in the years since Sauerbrey proposed the method, with reports[8] of sensitivities of better than 10^{-10} grams, equivalent to the resolution of a mass change due to the deposition of 0.16 Å of aluminum onto a 1 cm^2 surface.

Figure 2 is a block diagram of the quartz crystal film thickness monitor, or microbalance, built by this author. The electronics (Fig. 3) and the crystal holders (Fig. 4) were patterned after those of Waters and Raygor.[9] A single board contains the 10 MHz monitor and reference oscillators, the frequency mixer, and a one-stage output amplifier (Figs. 5 and 6). Both the reference and monitor crystals are housed in a single crystal holder, which is placed in the vacuum belljar next to the substrate onto which the amorphous transition

metal film is to be condensed. As the film condenses on the substrate and also on the near-by monitor crystal, the frequency of the monitor oscillator decreases. The mixer stage compares the monitor oscillator frequency to that of the reference oscillator by extracting a beat frequency from the two oscillator output signals. The beat frequency is amplified and measured with a frequency counter. This beat frequency is directly proportional to the mass of the film evaporated onto the crystal, and hence to its thickness. The reference and monitor crystal are housed in a single holder to minimize beat frequency shifts due to changes in crystal temperature.

Although the author completed two such microbalance circuits and demonstrated that the circuits and crystal holders function properly, difficulties were encountered in transmitting the 10 MHz rf signal from the electronics outside the belljar to the crystals inside the belljar. Time did not permit a resolution of these difficulties, and so the microbalance was not used for actual experimental measurements. Therefore, film thickness measurements were made using a Varian Å-Scope (model 980-4000) optical interferometer. Measurements made with this interferometer under near-ideal conditions have an accuracy of ±30 Å, but it was of course impossible to monitor film thickness during deposition.

B. Preparation of and Measurements on Amorphous $La_{.80}Ga_{.20}$ Films

Approximately 2 grams of $La_{.80}Ga_{.20}$ alloy were prepared by placing the pure La and Ga into a quartz tube and evacuating the tube to

~10^{-6} torr with a diffusion pump. The quartz tube was heated with a MAPP-gas torch until the metal was well melted and homogeneous.

The amorphous films were produced by the vapor quenching technique, in which an electron beam vaporizes a $La_{.80}Ga_{.20}$ sample resting in a water-cooled copper crucible with a tantalum inner-liner. (See Figs. 7, 8, 9, and 10.) The metal vapor strikes a glass substrate in thermal contact with a copper block, which is maintained at liquid nitrogen temperature (77°K). The metal vapor condenses on the glass substrate, but due to the low substrate temperature the metal atoms lack the mobility necessary to align into a crystalline structure.

The use of an electron gun for vaporizing alloys has distinct advantages over the use of a metal boat heated by passing electric current through the boat. The transition metals have high boiling points (~3000-5000°C), and frequently the melting point of the sample metal exceeds the melting points of commonly used resistive boats (which are themselves made from transition metals such as W, Ta, or Ti). The electron beam is capable of melting any metal, and furthermore its highly concentrated beam allows one to evaporate the surface of a sample without melting the bulk of the sample, eliminating the need for a crucible of high melting point. The high rate of energy deposition of the electron beam also allows one to evaporate an alloy without fractionation due to the differing vapor pressures of the component metals.

An ordinary glass microscope slide, 1" x 3", was used as a substrate. Gold pads were evaporated onto the slide to serve as

contacts for the resistivity measurements of the sample film (see Fig. 11(a)). These measurements were made by the standard 4-probe technique. Small (#44) wires were silver-painted to the gold pads. The slide was then mounted in a mask on the liquid nitrogen reservoir. A vacuum grease[10] of good thermal conductivity insured thermal contact between the glass slide and the copper block. A copper-constantan thermocouple mounted to the substrate holder was used to measure the substrate temperature.

A film mask insures that the sample film deposited over the gold pads has a well characterized geometry, as shown in Fig. 11(b). This is essential if one is to calculate the resistivity of the metal film from measurements of the film resistance and physical dimensions. The placement of the gold pads insures that the measurement of the film resistance is a measurement of only the long, narrow part of the film.

The sample film was evaporated in a high vacuum, 6×10^{-7} torr, to minimize impurities and oxidation of the film. Then the liquid nitrogen in the reservoir was removed, and the substrate allowed to warm slowly (~1°K/minute) from liquid nitrogen temperature (77°K) to room temperature (300°K). During this time, measurements of substrate temperature and film resistance were made in order to detect any sudden changes in resistance which would accompany a phase transition of the bulk of the film from the amorphous to a crystalline state. The resistance measurements were two-probe measurements made with a Keithley model 160B digital multimeter, with an error of approximately ±0.3%. The temperature measurements

were made by uncalibrated thermocouples having an absolute error of ±3°K, and a relative error between measurements of ±0.5°K. The reference thermocouple junction was immersed in a water-ice bath.

After the film reached room temperature, it was removed from the vacuum belljar and transferred to a helium cryostat for the transition temperature measurement. A schematic of the cryostat is shown in Fig. 12. The substrate is clamped to a copper block in thermal contact with a liquid helium reservoir (Fig. 13). By drawing a vacuum on the helium reservoir, the substrate can be cooled to ~1.5°K. The temperature of the substrate can then be slowly raised by means of an electric heater attached to the copper block. As this is done, an X-Y recorder plots the 4-probe resistance of the film as a function of the resistance of a calibrated germanium thermometer. From this plot, one can find the resistance of the film as a function of temperature, and thereby determine the superconducting transition temperature T_c. In the 1.5-15°K range, the Ge thermometer has an absolute accuracy of ±5 mdeg, and a relative accuracy of ±2 mdeg. However, the X-Y plotter introduces a greater uncertainty in the temperature.

After T_c was measured in the helium cryostat, the film was then placed in a pyrex tube filled with an argon atmosphere to prevent oxidation. The pyrex tube was placed in an electric oven, and heated at a rate of ~2°K/min from room temperature (300°K) to 500°K. Again, a 2-probe resistance measurement as a function of temperature was made to find any bulk phase transitions that might occur. If the

film is amorphous, one expects a sudden drop of about 10% in the film resistance at some point on the annealing curve, an indication that the film has crystallized. Also, one expects the slope $\frac{dR}{dT}$ to be negative for amorphous or possibly microcrystalline $La_{.80}Ga_{.20}$, whereas $\frac{dR}{dT}$ is positive for crystalline $La_{.80}Ga_{.20}$. Thus the slope of the annealing curve of the film can also provide some indications as to the nature of the film.

Lastly, the film and substrate are coated with a thin evaporated layer of aluminum in order to make the surface reflective. This is necessary to make the interferometer measurements of the thickness of the sample film. It has been shown that a thin aluminum coating will accurately follow the contour of the coated object, so that negligible error is introduced in the thickness measurement due to this aluminum overcoating.

III. Results and Interpretation of Data

Only two of the $La_{.80}Ga_{.20}$ films were produced, and complete data is not available for either film. For convenience, they shall be referred to as film #1 and film #2.

During the evaporation of film #1, one of the two leads connected to the contact pads broke, and so it was not possible to measure the resistance of the film as it warmed to room temperature.

Furthermore, a thermal shield in the He cryostat shifted during the measurement of T_c, cutting one of the four leads to the film. Thus, the resistance of film #1 was measured using 3 leads, rather than the more accurate 4-prove technique. The voltage drop across the film due to a constant 100 μa current in the film was measured with a Keithley 150B Microvolt Ammeter, and from this information the film resistance could be determined.

Figure 14 presents some representative data points on the transition curve for film #1. The author has adopted the convention that T_c is that temperature for which $\frac{R}{R_o} = .5$, where R is the resistance of the film as a function of temperature and R_o is the residual resistance of the film in the normal state. For film #1, $T_c = 4.71 \pm .03°K$. The largest contribution to the error of T_c is from reading the graph made by the X-Y plotter. Near T_c, the error in $\frac{R}{R_o}$ is estimated to be ±1.5%.

The transition curve of Fig. 14 is rather broad, with a particularly shallow slope in the region less than 5°k. This indicates that different portions of the film transist to the

superconducting state at different temperatures. One explanation would be that some portions of the film were amorphous or micro-crystalline, while other portions were crystalline. The differences in the T_c's of these different phases would cause the transition curve to "smear out", rather than be sharply defined.

Another explanation, which is more likely, is based on the condition of the gold pads. The gold contact pads of film #1 were deposited with the substrate at liquid nitrogen temperature. Films deposited on cold substrates are often brittle and crack easily. The gold pads for film #1 were observed to crack severely after deposition, and thus the pads were no longer electrically continuous. Thus the pads could not serve their intended purpose of acting as low resistance contact probes at the ends of the long, narrow part of the sample film (Fig. 11(b)). Instead, the resistance measurements now included the resistance of all of the sample film between the points at which the #44 wires for the voltage drop measurement were silver painted to the glass substrate.

Thus, the resistance of the sample film over the gold pads was included in the film resistance measurements. However, these regions of the sample film are expected to have a lower transition temperature than will portions of the film not over the gold pads. The reason for this is the proximity effect. The proximity effect occurs when a superconductor is in contact with a normal conductor (in this case, the discontinuous gold pads), with the result that the transition temperature of the superconductor is depressed. Thus, the transition

curve of Fig. 14 was probably "smeared out" due to the variations in the transition temperatures of regions of the film touching the gold pads.

No data is available on T_c for a crystalline $La_{.80}Ga_{.20}$ film, but the results of a recent study[11] of amorphous $La_{1-x}Ga_x$ films is partly summarized by Fig. 15. A value of $T_c = 3.8°K$ was reported for $La_{.80}Ga_{.20}$. Also from that same study, an annealing curve for amorphous $La_{.78}Ga_{.22}$ is presented (Fig. 16). Note the sudden drop in $\frac{R}{R_o}$ which shows the phase transition to the crystalline state. X-ray diffraction scans of the samples used in that study verify that the samples were indeed amorphous.

The annealing curve for film #1 is presented in Fig. 17. The scatter in the two points near 77°K is due to the inaccuracy of the thermocouple used to measure these two points, which was not in direct contact with the substrate. Between 4°K and 340°K the value of $\frac{dR}{dT}$ is clearly negative. This negative $\frac{dR}{dT}$ is consistent with the film being amorphous. However, the resistance began a dramatic rise at 340°K. This is believed to be due to oxidation of the film. This conclusion is supported by the fact that the film resistance continued its steep climb even when the film was cooled to room temperature again. The discontinuities in the graph at 345°K, 375°K, and 385°K are believed to be due to a loose contact lead, which also caused some momentary spurious meter readings. Possibly thermal stress on the film and silver paint are the cause of this.

Note that the lower sections of the discontinuities can be raised up to give a continuous curve from 345°K to 430°K. Thus, the drop at 345°K cannot be interpreted as a phase change, as might appear at first glance.

The thickness of film #1 is 3294 ± 112 Å based on 8 independent measurements. A calculation of the resistivity of the film at 6°K yields 723 ± 33 μΩcm. The expected resistivity for a film of these dimensions is ~200 μΩcm. The high value of measured resistivity could be due in part to film oxidation.

The experimental data on film #2 is rather sketchy. A breakdown in the electron gun controls resulted in a very thin film of high resistance (~3.5 kΩ). Figure 18 shows measurements made immediately after the film was produced. As the film was warmed from liquid nitrogen temperatures, it showed a strongly negative $\frac{dR}{dT}$, an excellent indication that the film was amorphous. However, a rise in resistance occurred at 210°K. This change was found to be irreversible, as shown by the arrows along the curve. However, the film still exhibited a negative $\frac{dR}{dT}$ of about the same slope as it first had. When the film was removed from the belljar, it was found that many small round holes existed in the film. A possible explanation is that prior to the evaporation, during which the sample to be evaporated was outgassed at very low beam power, gases condensed on the glass substrate which was at liquid nitrogen temperature. The $La_{.80}Ga_{.20}$ film was then deposited on the substrate, trapping the gas deposits. As the substrate was warmed,

the trapped gas deposits expanded until the film ruptured, pockmarking the otherwise continuous film and causing the rise in resistance. Some of the larger of these holes were perhaps as wide across as one-fourth the 0.756 mm width of the film, and could well account for the rise in resistance observed.

An attempt to measure T_c for film #2 was made, but the film broke at liquid nitrogen temperatures. Attempts to patch the discontinuities with silver paint failed. It was therefore also impossible to observe an annealing curve at greater than room temperature for film #2.

IV. Suggestions for Future Study

There are many possible suggestions for improving the experimental apparatus and technique. Implementing these suggestions would, however, raise the level of this research to the Master's level or higher. Some of the more obvious improvements are discussed below.

The films should be analyzed by x-ray or electron diffraction to determine the extent of disorder in the film. Also, an electron microprobe analysis of each film would be useful to determine the exact composition of the alloy of each film.

As these thin films can oxidize rapidly even in a good vacuum, it is desirable to make all measurements on a film as soon as possible. Because of the many transfers of the film between equipment, it would take at best two days of continuous work to make the measurements that were performed on film #1. As a result of equipment difficulties, it actually took six days of full-time work to complete the measurements on film #1, greatly increasing the possibilities of oxidation and crystallization. Therefore one would ideally make all measurements on the film without moving it from the apparatus in which it was evaporated. This would necessitate the design of a helium cryostat in which the evaporations could also be made.

In order to prepare a wide range of alloys, it is also desirable to evaporate the alloy components simultaneously from separate crucibles, and to be able to control the rate of deposition of each component. This requires measurements to be made

with a quartz crystal microbalance for each component metal. The information from the microbalance would be used to control the electron guns performing the evaporation. A shutter should be placed over the film substrate, allowing one to outgas the samples and adjust the evaporation rate before opening the shutter and producing a film. Lastly, the breakage of leads can cause considerable problems, thus redundant leads should be used whenever possible to insure that valuable data on a film will not be lost in the event that one lead breaks.

V. Conclusion

A $La_{.80}Ga_{.20}$ film 3294 Å thick was produced and was found to have a T_c of 4.71°K, and a residual resistivity of 723 μΩcm at 6°K. The annealing curve for this film is incomplete, but does suggest a negative $\frac{dR}{dT}$ indicating that the film, or parts of it, were probably amorphous. The annealing curve of a second film also indicates that it remained amorphous at least up to a temperature of 250°K, but there is no conclusive evidence that either film remained truly amorphous at room temperature. The rapid oxidation and subsequent destruction of these films presents great difficulties in making the required measurements.

The results presented here should be considered only as trial runs during which the equipment and techniques were debugged, and no attempt is made to represent the measured T_c as an accurate measurement for an amorphous film. However, the feasibility of the system has been demonstrated, and the problems encountered and experience gained with this system will benefit the current project of one of the physics graduate students, who will refine the apparatus and continue the study of amorphous transition metals.

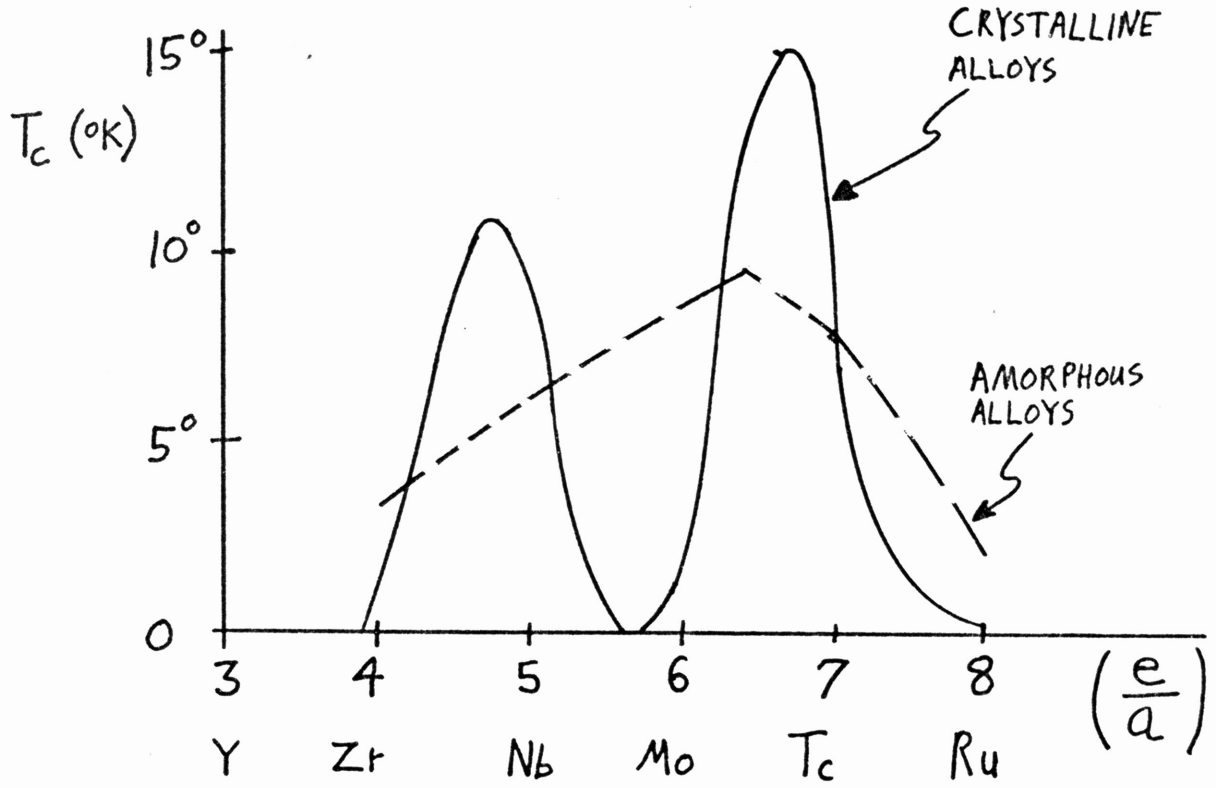

Fig. 1. Superconducting transition temperatures are shown as a function of the average number of valence electrons per atom for alloys of 4-d transition metals. A comparison is drawn between the behavior of crystalline films (solid line) and amorphous films (dashed line). The minimum near $\frac{e}{a} = 6$ in the T_c's of crystalline films has been explained as due to the formation of directed d-bonds between atoms. These d-bonds cannot form in an amorphous film.

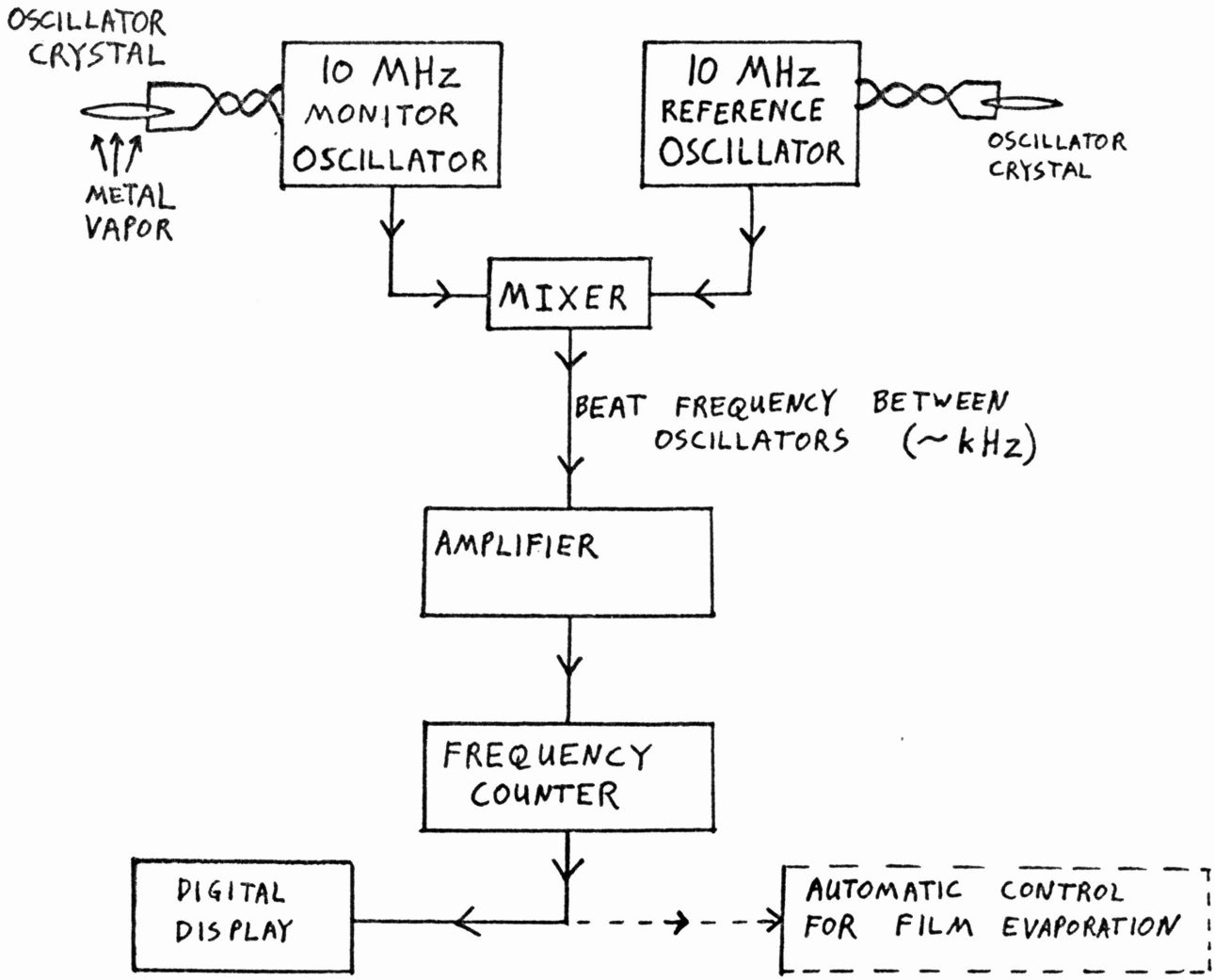

Fig. 2. Block diagram of quartz crystal film thickness monitor. Mass loading on the crystal of the monitor oscillator lowers its resonant frequency. This frequency is beat against a 10 MHz reference signal to reduce the information to a more easily measured form. The beat frequency is directly proportional to the mass added to the crystal, and therefore to the thickness of the film deposited on the crystal. The addition of 1 Å of aluminum causes a change of ~6 Hz in the beat frequency.

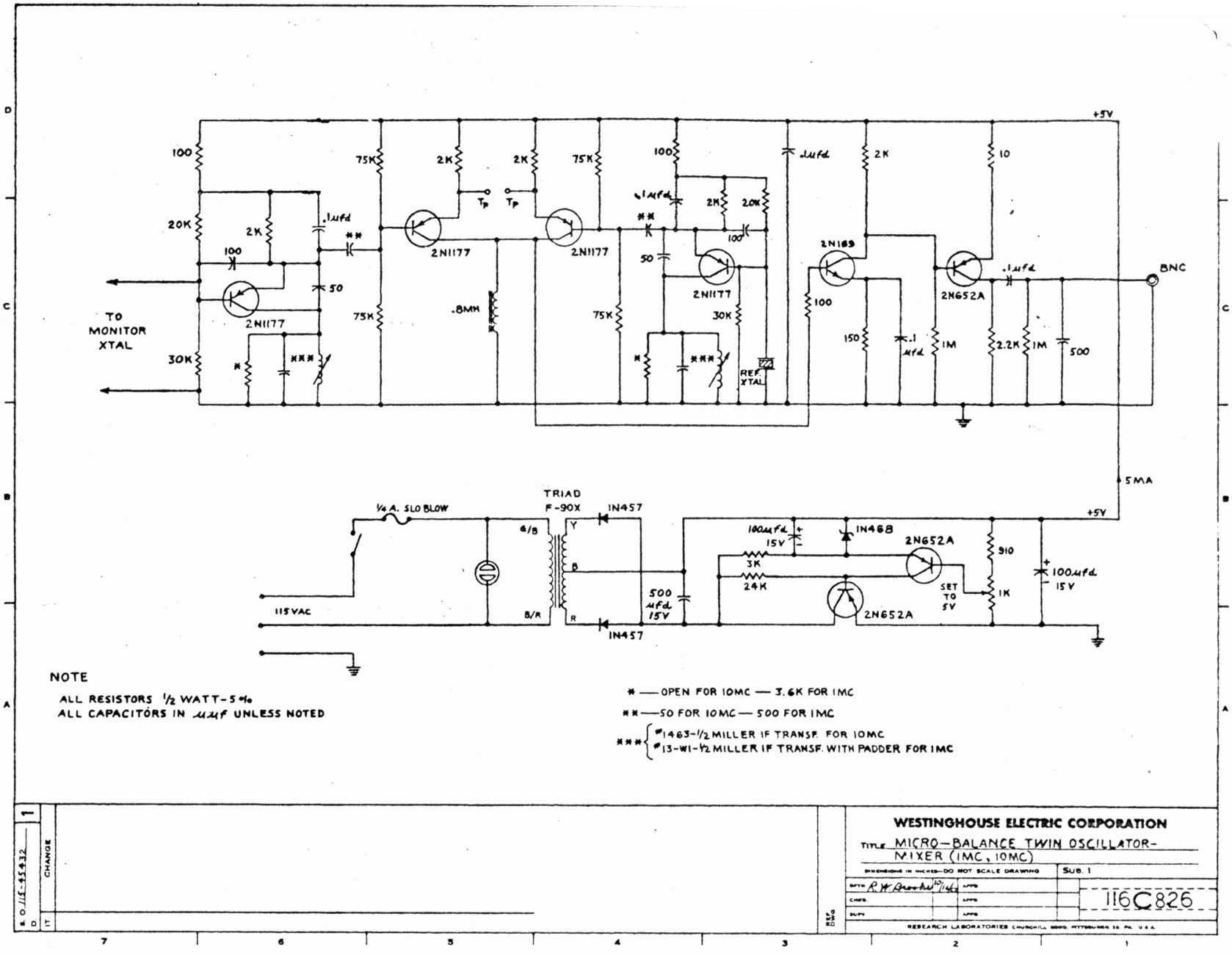

Figure 3

Schematic diagram of dual oscillator-mixer and power supply. Starred items are selected on the basis of operation at either 1 or 10 Mc.

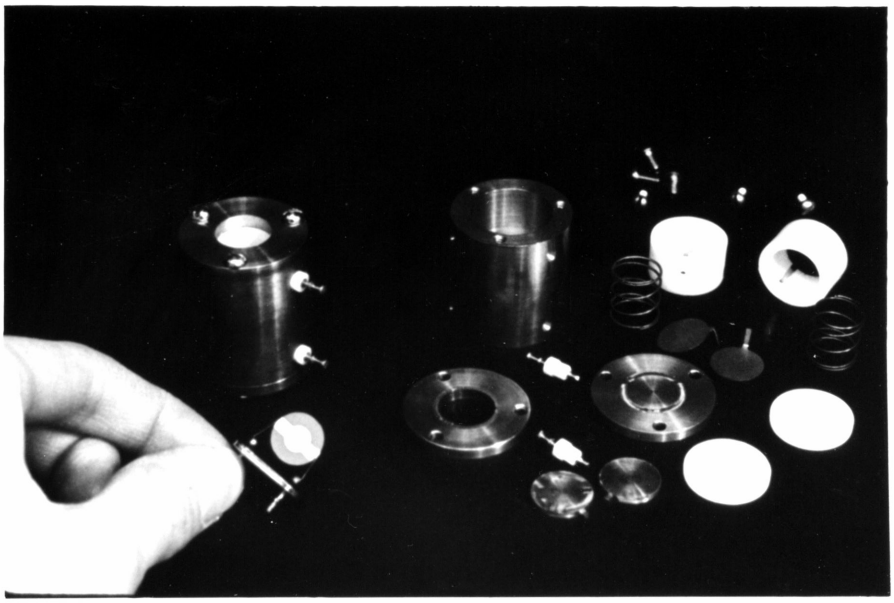

FIG. 4. Crystal holders for a quartz crystal microbalance. The hand holds a commercial 10MHz mounted radio crystal. Directly above the hand is an assembled microbalance 10MHz crystal holder containing both the reference crystal and monitor crystal. The monitor crystal is seen exposed by an aperature on the top end of the holder. The disassembled parts of a second crystal holder are shown on the right hand side of the photo. Construction is primarily of copper and teflon.

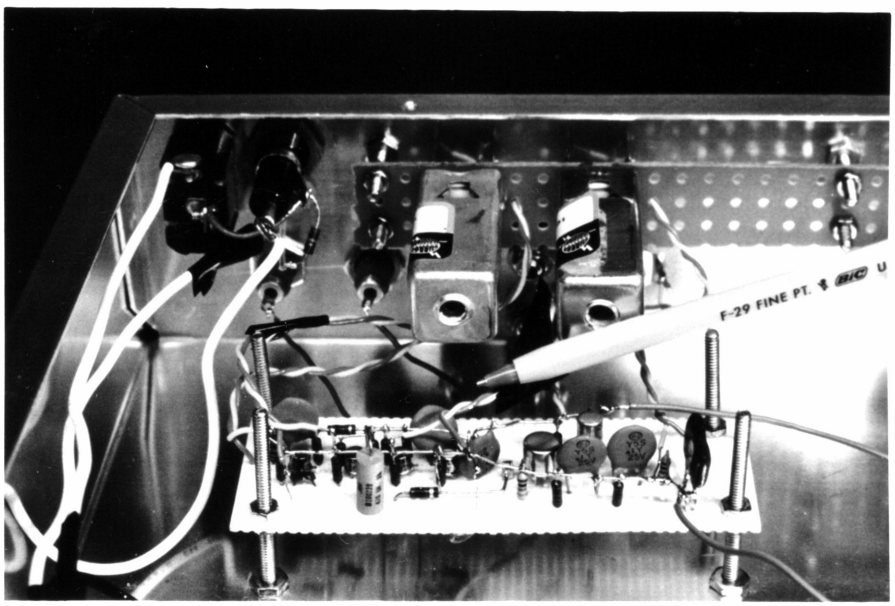

FIG. 5. Microbalance circuit. A single board holds the reference and monitor oscillators, signal mixer, and amplifier. The two metal cans above the circuit are tuneable tank circuits for the oscillators. Close component placement is critical in the high frequency portions of the circuit.

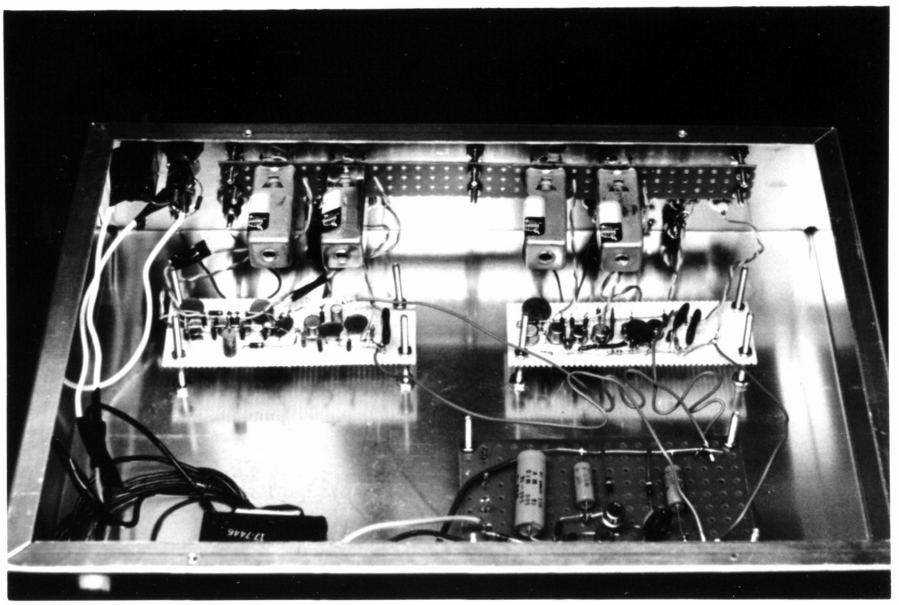

FIG. 6. Two microbalance circuits with regulated power supply. The author built these in anticipation of evaporating the alloy components separately but simultaneously, and controlling the alloy composition during evaporation.

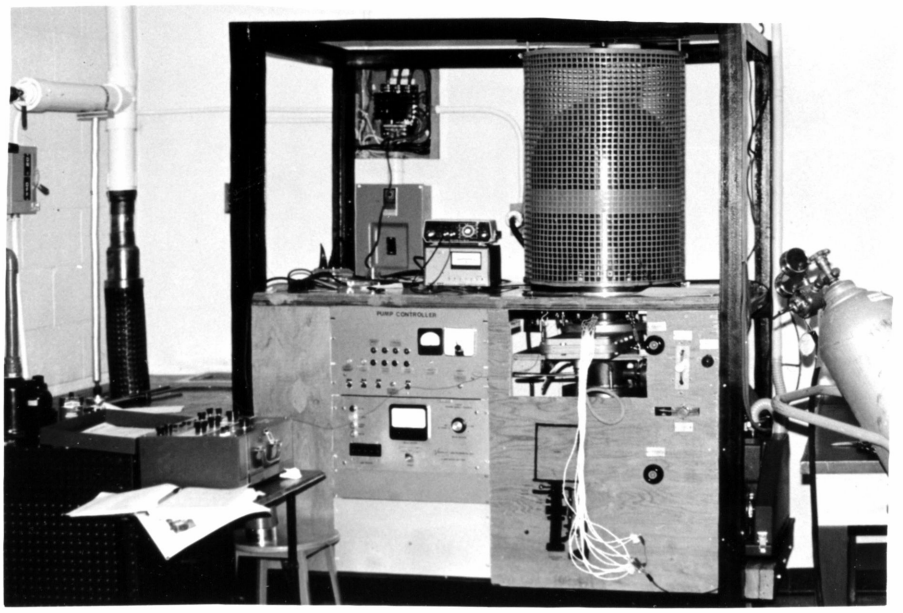

FIG. 7. Vacuum belljar for thin film evaporations. A precision millivolt galvanometer for thermocouple measurements rests on the table to the left. Controls for the pumps and electron gun are mounted on the belljar mainframe. The large circuit breaker boxes in the background are indicative of the large power requirements of the electron gun.

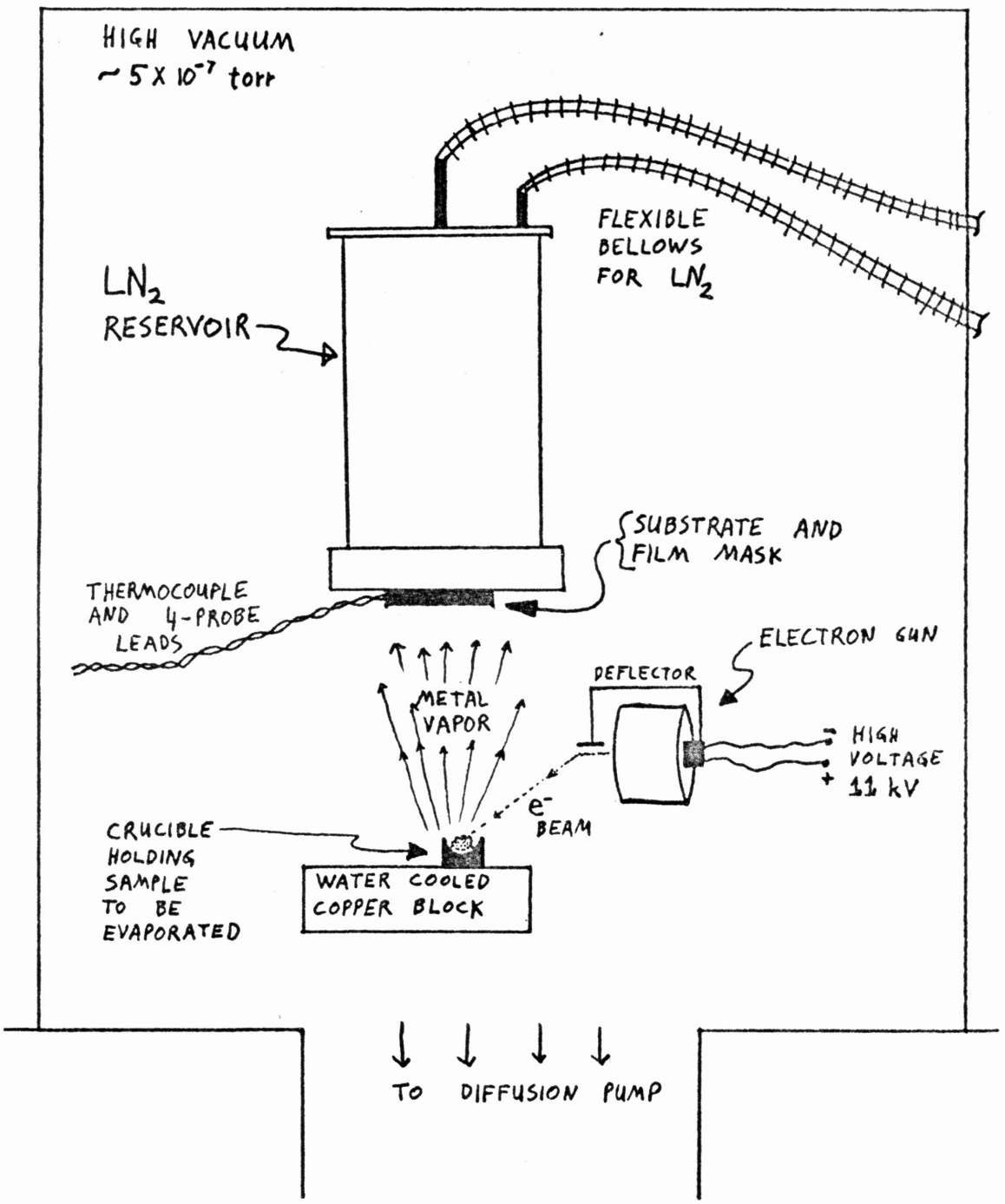

Fig. 8. The author's experimental apparatus for producing thin amorphous metal films by the vapor-quench technique. Liquid nitrogen for the reservoir and cooling water for the target block may be introduced into the belljar without breaking the vacuum. Compare with Figs. 9 and 10.

FIG. 9. Vapor-quench film production apparatus. The large cylinder in the center is the LN_2 reservoir with the LN_2 bellows entering at its top. The substrate holder is visible, and is bolted to the bottom of the reservoir. The electron gun is to the lower right of the reservoir. The water cooled target block and crucible are below and to the left of the gun. (See FIG. 10)

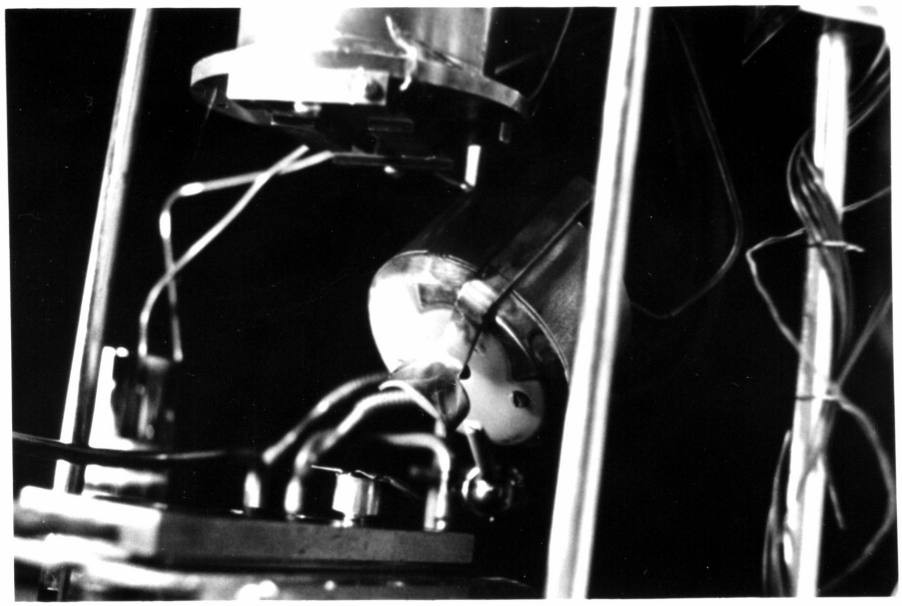

FIG. 10. Two photographs of the electron gun, water cooled target block and crucible, and the substrate holder on the LN_2 reservoir. The electron aperature in the center of the gun face is clearly seen in the photo on the left. The round crucible is threaded to screw in and out of the holes on the water cooled copper block.

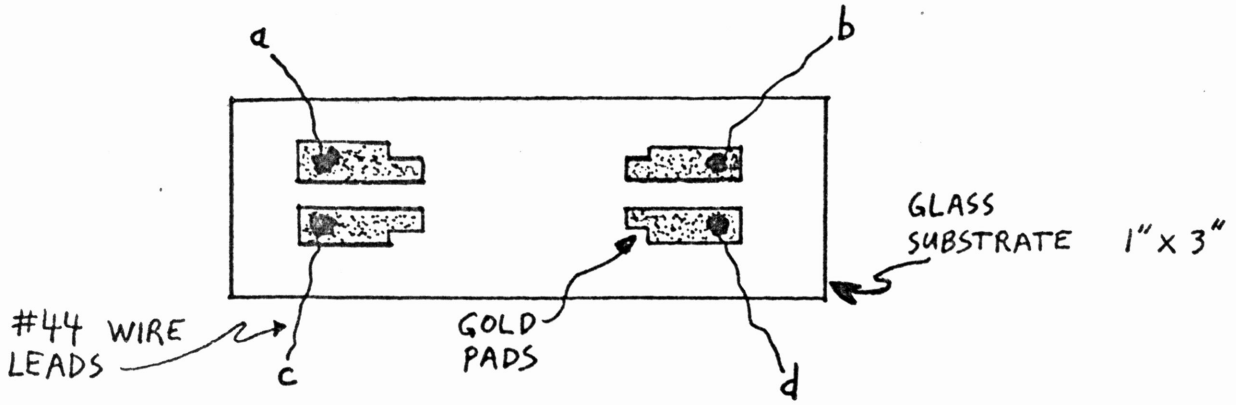

Fig. 11a

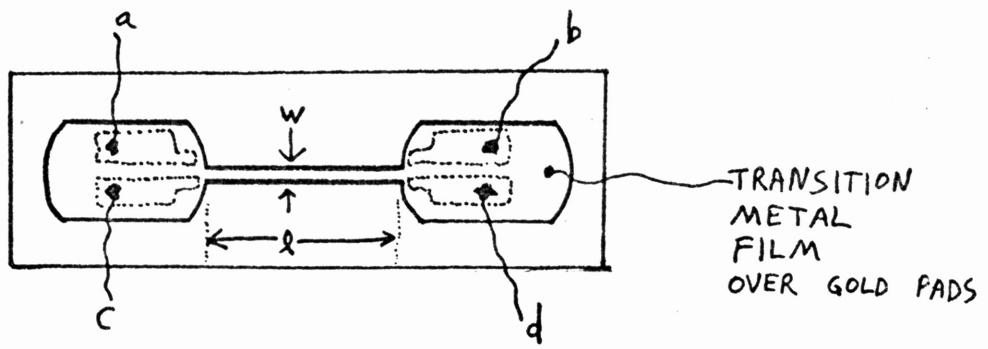

Fig. 11b

Fig. 11. (a) Shows the glass slide with gold contact pads. #44 wires (a,b,c, and d) are attached to the pads by silver paint.
(b) Shows the geometry of the sample film deposited over the gold pads. The 4-probe resistance measurement involves sending a constant current through leads a and b. The voltage drop across c and d is measured. In this manner, the resistance R=V/I of the narrow strip of length ℓ= 2.4431 cm and width w = 0.756 mm is measured. The resistivity ρ of this strip is determined by $R = \frac{\rho \ell}{wd}$, where d is the film thickness, and ρ has the units $\mu\Omega$cm.

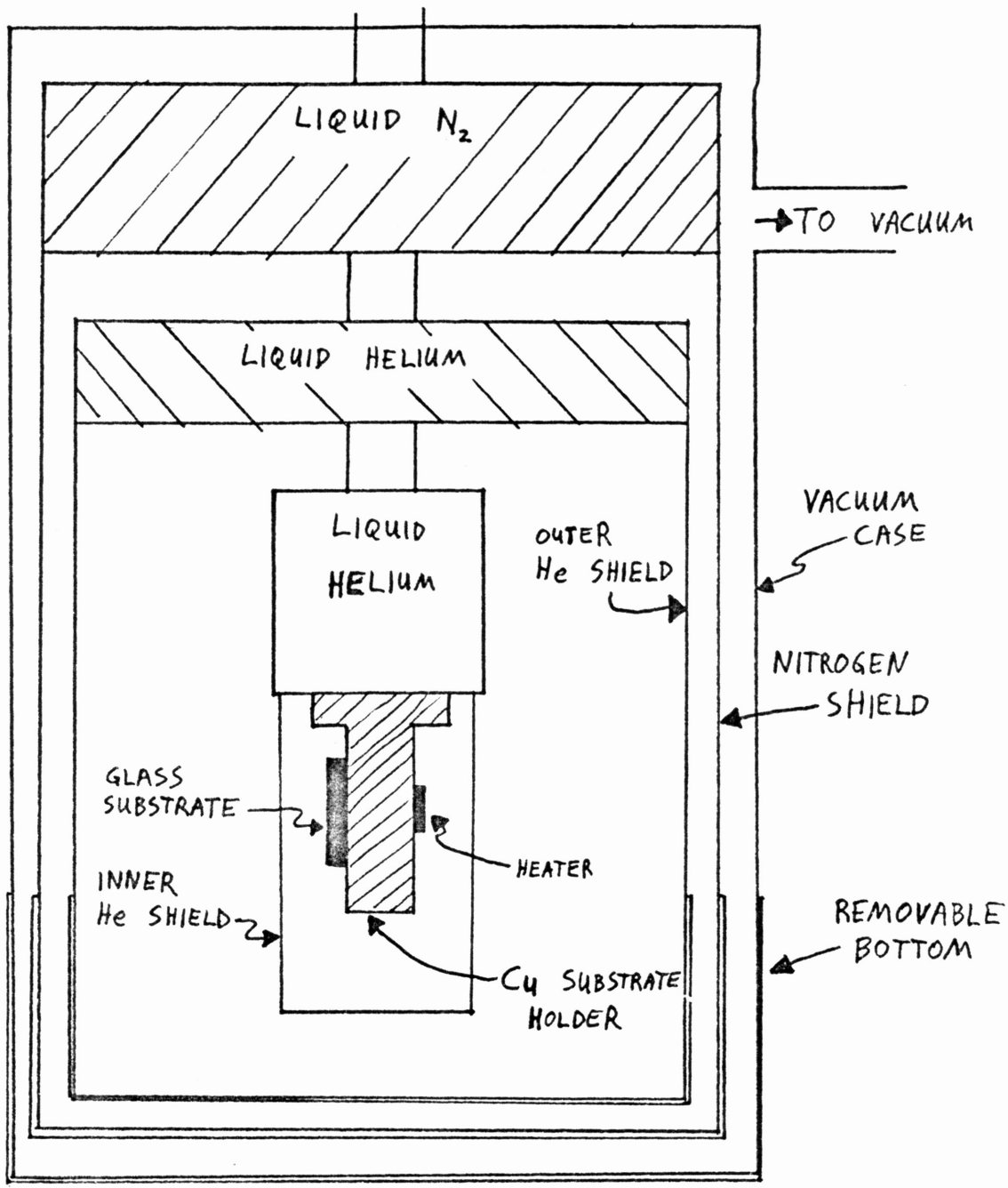

Fig. 12. Helium cryostat for transition temperature measurements. Temperatures ~1.5°K may be attained. The nitrogen and helium shields screen out thermal radiation.

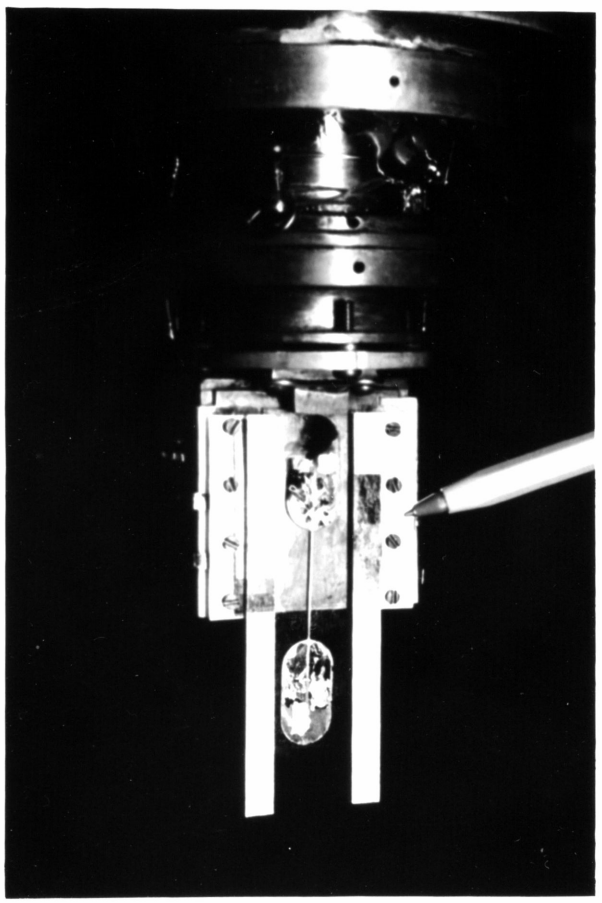

FIG. 13. A glass substrate with film is seen mounted on the lower helium dewar of the helium cryostat (see FIG. 12). The gold pads underneath the film appear as discolored areas in the oval ends of the film. (Refer to FIG. 11).

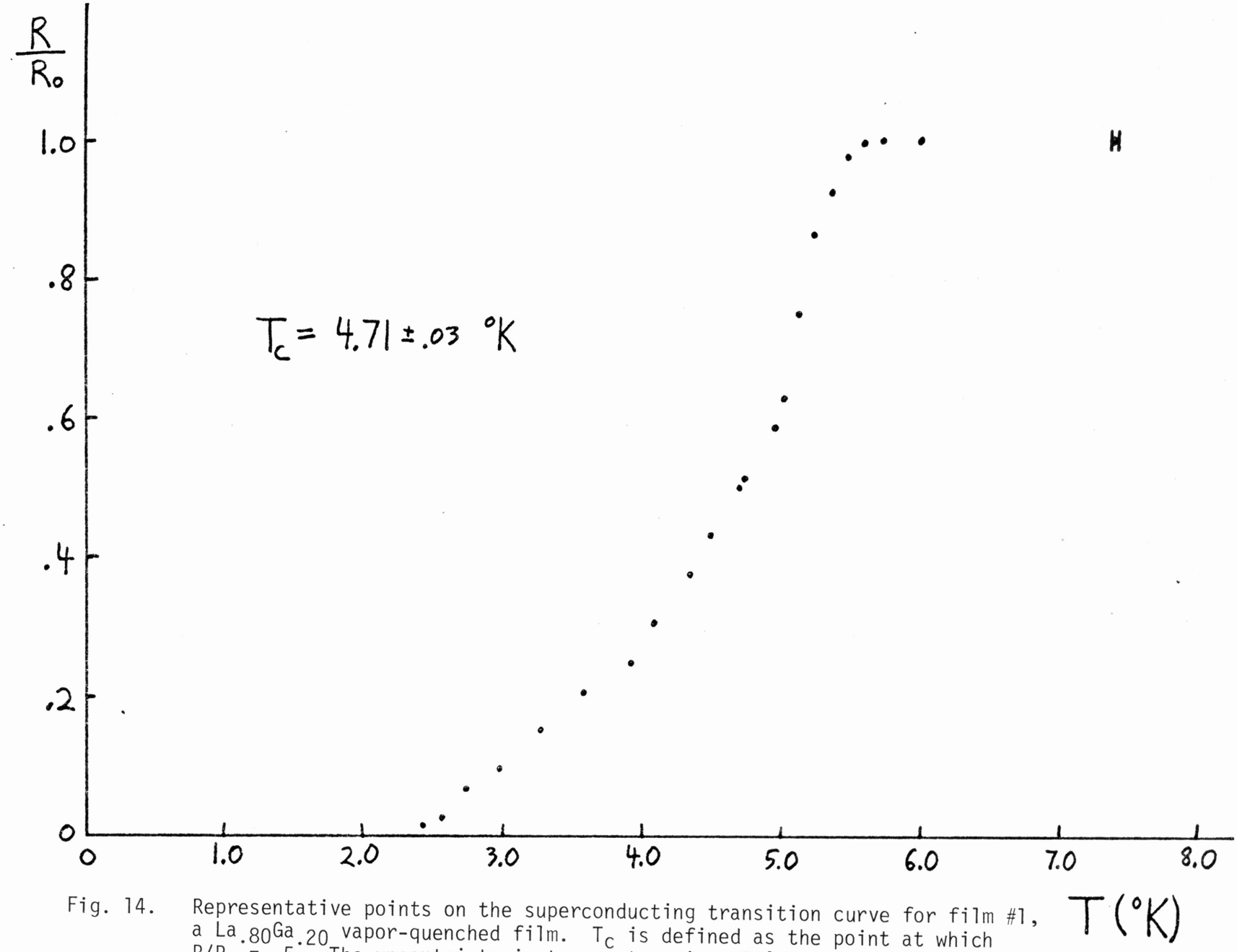

Fig. 14. Representative points on the superconducting transition curve for film #1, a $La_{.80}Ga_{.20}$ vapor-quenched film. T_c is defined as the point at which $R/R_0 = .5$. The uncertainty in temperature is ±.03°K, the uncertainty in R/R_0 near T_c is ±1.5%. The residual film resistance at 6°K is $R_0 = 708.9\ \Omega$.

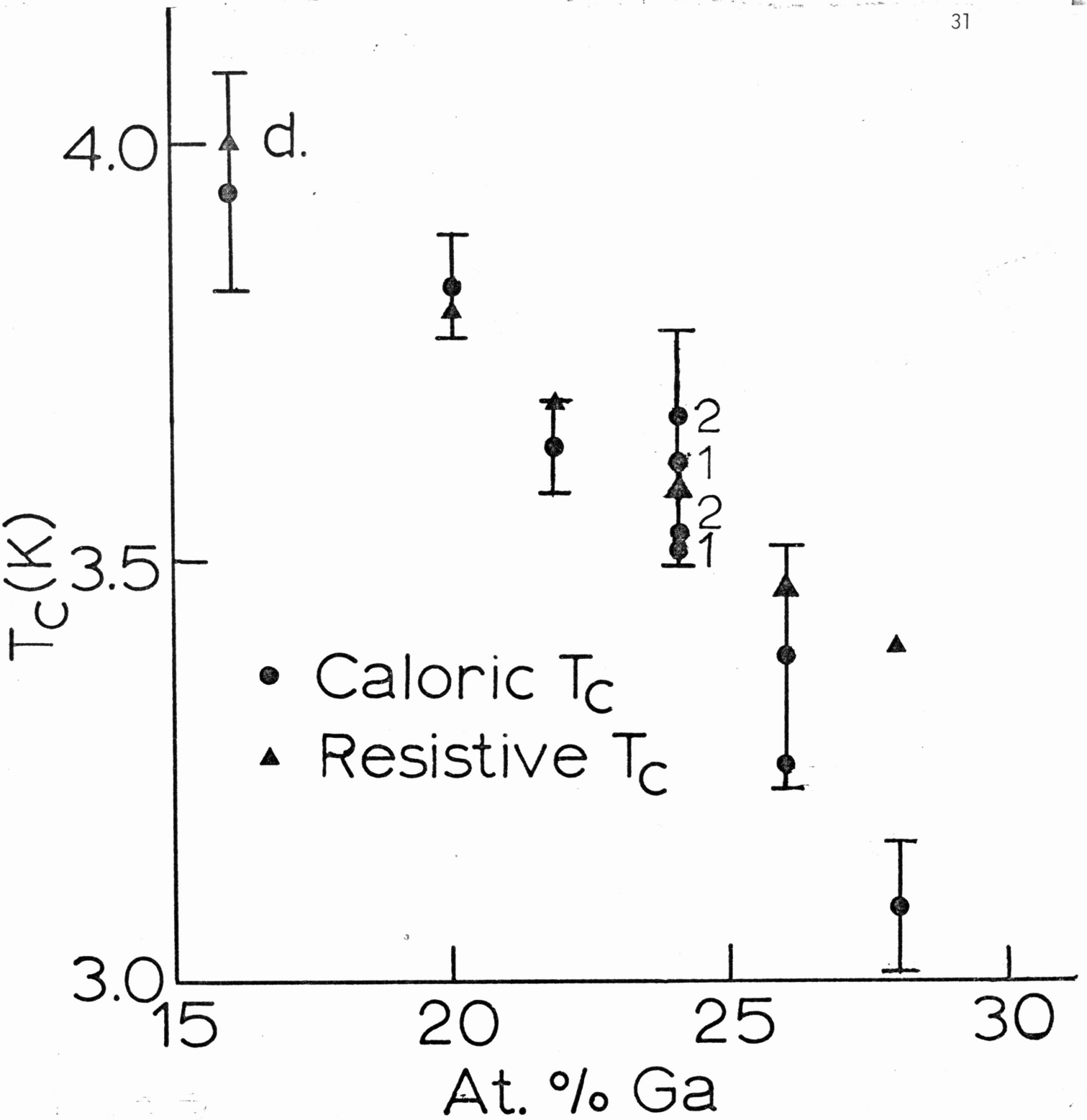

Fig. 15. Superconducting transition temperatures for $La_{1-x}Ga_x$ splat-cooled foils are shown as a function of atomic percent Ga.

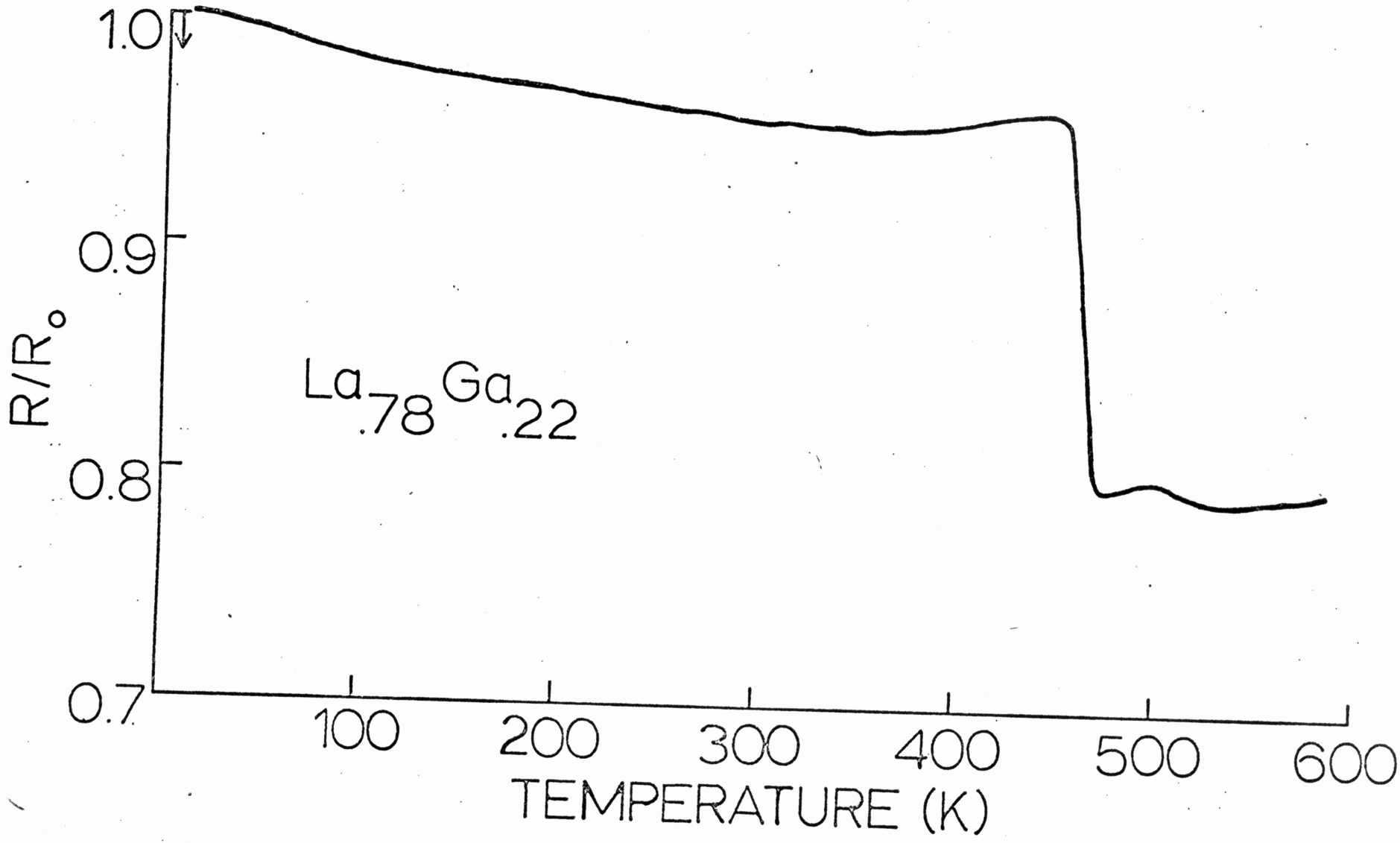

Fig. 16. An annealing curve for an amorphous $La_{.78}Ga_{.22}$ splat-cooled foil. The sudden drop in resistance at 450°K corresponds to a phase transition from the amorphous to the crystalline state. Note that dR/dT is negative for the amorphous metal.

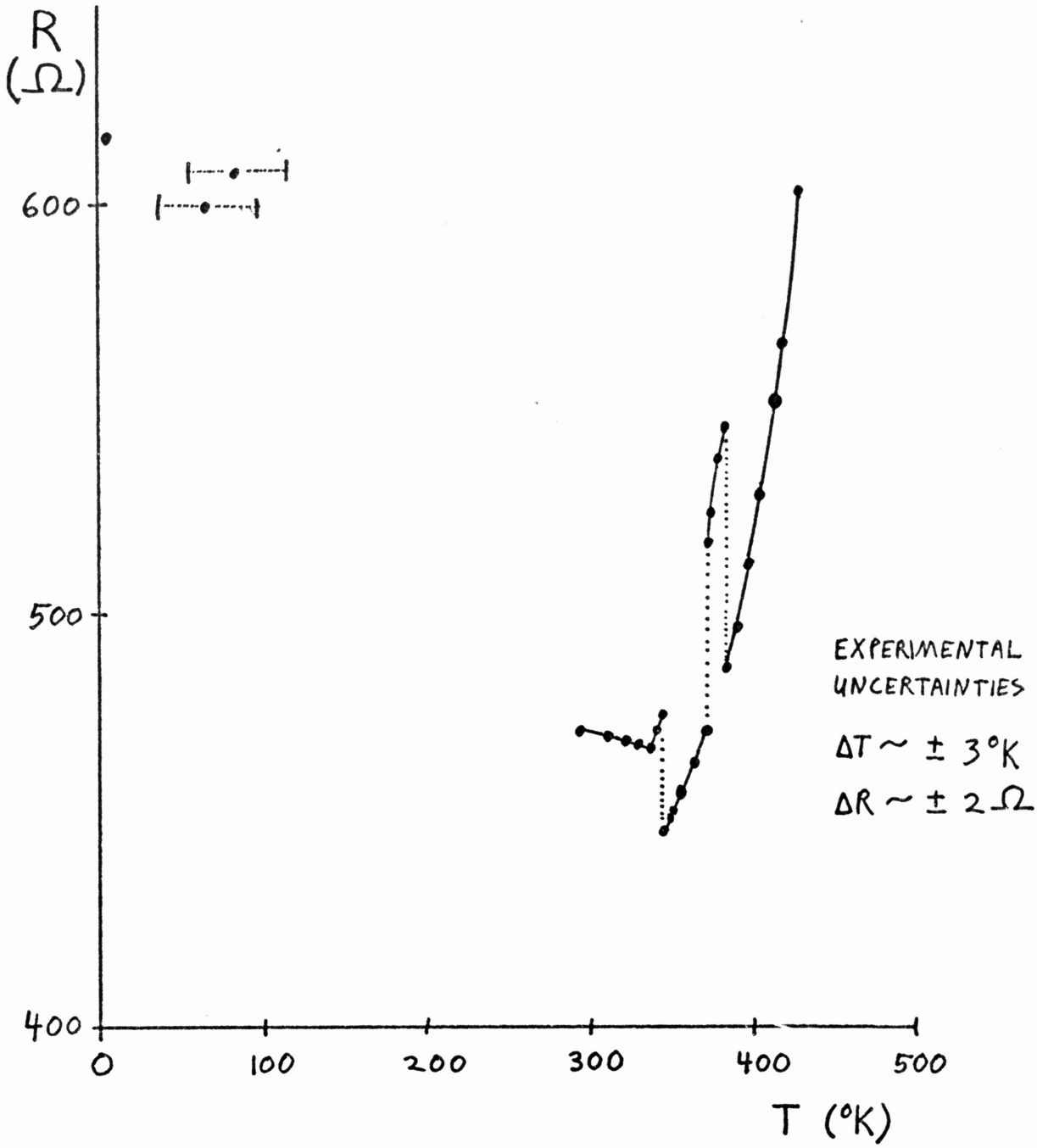

Fig. 17. Annealing curve for film #1, a $La_{.80}Ga_{.20}$ vapor-quenched film. The discontinuities in the curve between 300°K and 400°K are believed due to a loose contact wire. The sharp rise in resistance beginning 340°K is believed due to the film oxidation. Nevertheless, the curve remained smooth due to a constant rate of temperature increase.

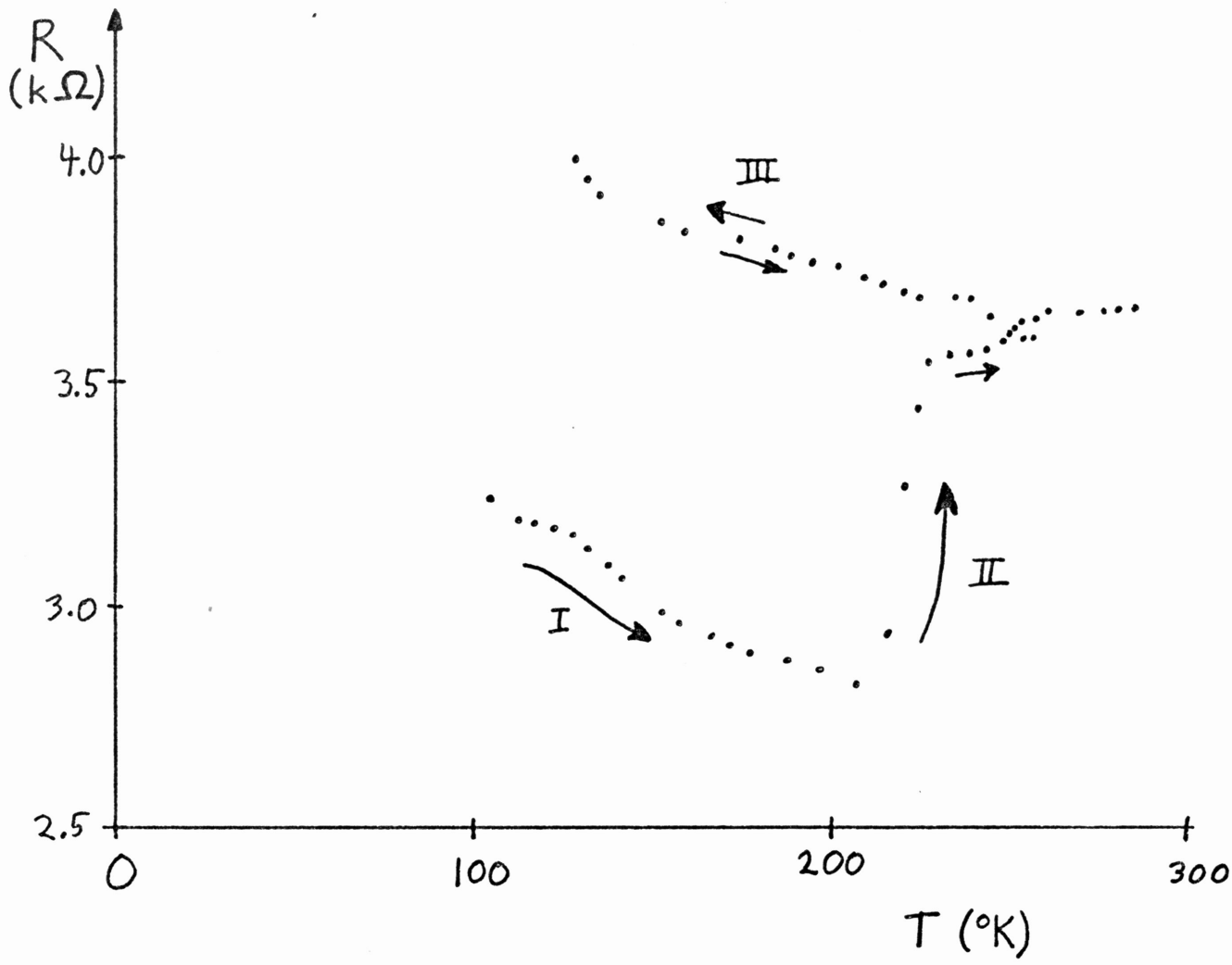

Fig. 18. Annealing curve for film #2, a $La_{.80}Ga_{.20}$ vapor-quenched film. Curve I was taken immediately after the film's production at 77°K. Curve II is an irreversible increase in resistance that occurred during the initial warm-up of the film. Curve III contains points taken as the film was re-cooled to 77°K and then warmed again. Notice that dR/dT is negative for both I and III, which is consistent with the $La_{.80}Ga_{.20}$ film being amorphous. Uncertainties in temperature are ±3°K absolute, ±0.5°K relative. Error in R is ±2Ω.

REFERENCES

1. W. Buckel and R. Hilsch, Z. Physik 138, 109 (1954).
2. G. Bergmann, Phys. Rep. 27C, 159 (1976) presents a survey of experimental results.
3. M. M. Collver and R. H. Hammond, Phys. Rev. Letters 30, 92 (1973).
4. B. T. Matthias in The Science and Technology of Superconductivity, Vol. 1, edited by W. D. Gregory, et al., Plenum Press, New York, 1973.
5. W. H. Shull, D. G. Naugle, S. J. Poon, and W. L. Johnson, paper submitted to Phys. Rev.
6. P. Duwez, R. H. Willens, and R. C. Crewdson, J. Appl. Phys. 36, 2267 (1965).
7. G. Sauerbrey, Physik Verhand. 8, 113 (1957).
8. P. M. Waters and P. O. Raygor, Westinghouse Research Report 62-115-454-R2, (1962).
9. P. M. Waters and P. O. Raygor, Westinghouse Research Report 62-115-454-R2, (1962).
10. Apiezon N vacuum grease, distributed in the U.S.A. by James G. Biddle Co., Plymouth Meeting, Pa., 19462.
11. W. H. Shull, D. G. Naugle, S. J. Poon, and W. L. Johnson, paper submitted to Phys. Rev.